JACS
JOURNAL OF THE AMERICAN CHEMICAL SOCIETY

Communication

pubs.acs.org/JACS

On the Remarkable Role of Surface Topography of the Bottom Electrodes in Blocking Leakage Currents in Molecular Diodes

Li Yuan,[†] Li Jiang,[†] Damien Thompson,[‡] and Christian A. Nijhuis*[,†,§]

[†]Department of Chemistry and [§]Graphene Research Centre, Solar Energy Research Institute of Singapore, National University of Singapore, Singapore 117543

[‡]Materials and Surface Science Institute and the Department of Physics and Energy, University of Limerick, Ireland

Supporting Information

ABSTRACT: It was proposed in 1974 that molecules could rectify, but molecular diodes with simultaneously high rectification ratios, yields of working junctions, and reproducibility are rare, despite a huge body of experimental work. Although every type of molecular junction contains a certain distribution of defects induced by the topography of the surface, the roles of these defects in the device performance are rarely studied. We show that control over the topography of the bottom electrode in self-assembled monolayer (SAM)-based junctions in terms of the number of grains, the width of the grain boundaries, and the roughness improves the yield of working junctions from 60% to near 100%, increases reproducibility by a factor of 3, and boosts the rectification ratio of a molecular diode (from nearly unity to $\sim 1.0 \times 10^2$) by minimizing the leakage currents. We found that commonly used metal surfaces fabricated by direct deposition methods are inferior to template-stripped surfaces, which are flat and contain only small areas of exposed grain boundaries, at which SAMs cannot pack well. Thus, for molecular diodes to perform well, it is crucial to minimize leakage currents by limiting the amount of exposed grain boundaries.

Molecular electronics aims to generate devices with electrical characteristics that are determined by the chemical and supramolecular properties of the molecules.[1] This goal has been difficult to achieve, as uncertainties in the (supramolecular) structure of the junctions caused during the fabrication process can be a source of artifacts hampering the interpretation of the data and the performance of the devices. Here we show that control over the surface topography of a silver bottom electrode that supports a self-assembled monolayer (SAM) of $S(CH_2)_{11}Fc$ ($\equiv SC_{11}Fc$; Fc = ferrocene) in contact with top electrodes of Ga_2O_3/EGaIn (eutectic alloy of In and Ga with a 0.7 nm surface layer of Ga_2O_3)[2] allowed us to improve four characteristics of these SAM-based molecular diodes: (i) the yield in working and stable junctions increased from 60% to 95%, (ii) the reproducibility (log-standard deviation) improved by a factor of 3, (iii) the leakage currents decreased by nearly 2 orders of magnitude, and (iv) the rectification ratio R increased from nearly unity to 1.0×10^2. R is given by eq 1, where $|J(-1.0\ V)|$ and $|J(+1.0\ V)|$ are the current densities, in A/cm^2, measured at −1.0 and +1.0 V. Here we define the leakage current as the value of J that flows across the diodes at +1.0 V when they are in the "off" state and block the current; the diodes allow the current to pass through at −1.0 V when they are in the "on" state.

$$R = \frac{|J(-1.0\ V)|}{|J(+1.0\ V)|} \quad (1)$$

To control electronic function in molecular junctions, e.g., negative differential resistance,[3] switching,[4] and memory,[5] the emphasis has been on the chemical structure of the organic component, but it has been challenging to prove whether the electronic function was molecular in origin or because of, for instance, filaments[6] or chemical side reactions.[3b] For example, molecular diodes made of complex molecules containing donor-bridge-acceptor groups (D-b-A)[7] have been studied since the original proposal by Ratner and Aviram,[8] but it is difficult to control the supramolecular structure of SAMs composed of these molecules. Consequently, physical-organic studies of charge transport across them have been challenging.[9] Indeed, most studies involving junctions incorporating D-b-A compounds rectified currents with low values of $R < 10$.[7,10] As we show here, defects induced by grain boundaries cause large deviations from the "ideal" supramolecular structure of the SAMs. Consequently, the performance of molecular diodes composed of the same chemical structure changes from resembling that of a "good diode" to that of a "nonworking diode" upon changing the topography of the bottom electrode that supports the SAM. The details of the fabrication of the bottom electrode are of crucial importance, and a good understanding of the role of defects is required in order to discriminate artifacts from real data.

Common defects in metal surfaces can easily exceed molecular dimensions (see below). Whitesides et al.[11] showed that limiting the number and size of defects is important to improve the reproducibility of SAM-based junctions. Very recently, we showed that the surface topography affects the tunneling decay coefficient β (in Å^{-1}).[12] Both studies involved only junctions with SAMs of SC_n, making it difficult to determine how surface-induced defects affect leakage currents and the electronic performance of junctions, such as molecular diodes.

Figure 1 shows schematically a Ag^{TS}-$SC_{11}Fc$//Ga_2O_3/EGaIn junction that contains grains. Figure 1D shows an atomic force microscopy (AFM) image of an annealed, template-stripped (A-TS) silver surface with large grains and typical defects such as grain boundaries and step edges. On a grain, SAMs can form with

Received: January 22, 2014
Published: April 16, 2014

   dx.doi.org/10.1021/ja5007417 | J. Am. Chem. Soc. 2014, 136, 6554−6557

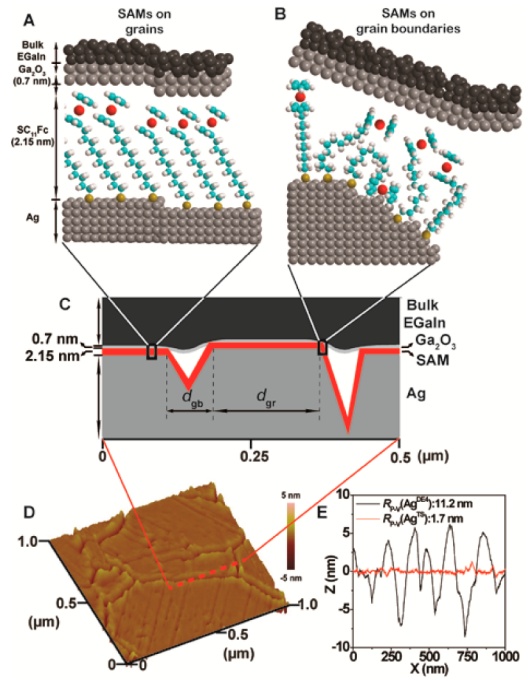

Figure 1. Schematic illustration of the junction of $Ag^{A\text{-}TS}$-$SC_{11}Fc$//Ga_2O_3/EGaIn with the SAMs formed on a grain (A) and at a grain boundary (B). Simplified illustration of a part of the junction (C) based on a line scan as indicated in the AFM image of a $Ag^{A\text{-}TS}$ surface (D). The arrows indicate the width of the groove between two grains (d_{gb}) and the distance between two grain boundaries (d_{gr}). Typical line scans for Ag^{TS} and Ag^{DE4} surfaces (E).

"perfect" structure (Figure 1A) but are more liquid-like and defective at grain boundaries (Figure 1B). Figure 1A illustrates how SAMs on grains can still have defects caused by, for instance, step-edges and phase domain boundaries, but AFM line scans in Figures 1E and S1 (Supporting Information) show that the width and depth of the grain boundaries are larger than the molecular dimensions. At these defect sites the SAMs cannot pack well, which lowers the distance between the two electrodes, d (in nm).[11] The measured current density has an exponential dependence on d, as described by the simplified Simmons equation (in the low bias limit, eq 2), where J_0 is the current

$$J = J_0 \, e^{-\beta d} \tag{2}$$

density for the junction with d = 0 nm. Thus, the measured tunneling current is very sensitive to defects that reduce d (regardless of the tunnel pathway, e.g., through-space or through-bond[11]) and exponentially increase of the value of J. Here we show that, by minimizing the presence of grain boundaries, one can obtain junctions with electrical characteristics that are dominated by the supramolecular properties of the SAM.

We reported previously that junctions of the form Ag^{TS}-$SC_{11}Fc$//Ga_2O_3/EGaIn have rectification ratios $R \approx 1.0 \times 10^2$, which are large enough to conduct physical-organic studies.[13,15] The mechanism of charge transport across these junctions has been described in detail elsewhere; the rectification is induced by the asymmetry of the molecule and not by any of the other asymmetries present in the junction, nor the conductive layer of Ga_2O_3.[13,14] Here we use this model system to study how R, yield in working junctions, current densities, and reproducibility (or the log-standard deviations) vary with the topography of the bottom electrode. We control four factors that are important in the topography of the surfaces: (i) the number of grains, N_{gr}; (ii) the width of the groove between two grains, d_{gb} (in nm); (iii) the area of the grain boundaries, A_{gb} (in μm^2); and (iv) the root-mean-square (rms) roughness (over an area of 5.0 × 5.0 μm^2). AFM was used to analyze the topography of the bottom electrodes (Table S1). The value of A_{gb} directly relates to the area of the grain boundary A_{gr} (surfaces with small grains have more grain boundaries than those with large grains) and was estimated from A_{gr} and the value of d_{gb} (obtained from line scans) after normalization for the N_{gr} (see SI for details) following a previously reported procedure.[12] The grains do not need to be in a single plane, which largely determines the rms value. To capture these factors in a single parameter, we estimated the bearing volume, BV (in nm^3), using eq 3. Surfaces with large BV values are rough and defective, and have a large fraction of exposed grain boundaries, while the opposite is true for surfaces with low BV values.

$$\mathrm{BV} = N_{gr} A_{gb} \mathrm{rms} \tag{3}$$

We used four common methods to prepare bottom electrodes: (i) template-stripping (Ag^{TS}), (ii) combination of annealing and template-stripping ($Ag^{A\text{-}TS}$), (iii) direct deposition (Ag^{DE}) on Si/SiO_2, and (iv) germanium-seeded growth of 15 nm Ag (Ag^{SD}).[16] By controlling the deposition rate, the rms value of the DE surfaces could be controlled from 1.2 to 5.1 nm. Figures 2 and S1 show the AFM images of these surfaces.

Figure 2 shows the average J−V curves and the histograms of the values of R_{tot} with Gaussian fits to these histograms (see discussion below). Junctions with SAMs of $SC_{11}Fc$ on $Ag^{A\text{-}TS}$ and Ag^{TS} surfaces had the highest R_{tot} values, ~1.0×10^2, while junctions with Ag^{DE} surfaces had poor device characteristics and the value of R_{tot} dropped to nearly unity as a function of BV (Table S2). The Ag^{SD} surface, i.e., the surface with the smallest A_{gr} and rms, resulted in a single and narrow peak centered at R_{tot} = 20. Although R_{tot} is modest, these junctions have the highest reproducibility, defined as the log-standard deviation, σ_{log}, of the log-average, μ_{log}, of R_{tot}.

We fitted to the histogram of R one Gaussian to obtain R_G (see Figure S3). This method resulted in poor fits for the DE surfaces because the histograms of R show that the distributions consist of two main peaks. Therefore, we used two Gaussians to fit the data to obtain R_1 and R_2, and the total value of $R_{tot} = R_1 \times R_1\% + R_2 \times R_2\%$ (with their relative surface areas expressed as a percentage) is similar to R_G (Table S2). We assign R_1 to junctions that are dominated by "ideal" structures and the top electrode mainly probes SAMs on grains, and R_2 to junctions that are dominated by disordered structures and the top electrode mainly probes SAMs at grain boundaries, as depicted in Figure 1, for five reasons. (i) The A-TS and TS surfaces have large values of A_{gr} and therefore small values of d_{gb}, resulting in a small value of BV (see Table S1). The conformable top electrode therefore probes predominantly SAMs on grains, and R_1 dominates the distribution. (ii) The DE surfaces have small values of A_{gr} but d_{gr} values are similar to those of the TS surfaces, resulting in large BV values. The top electrode therefore probes significant amounts of disordered SAMs on grain boundaries, and R_2 dominates. (iii) The area of R_2 increases while that of R_1 decreases with increasing BV for a series of DE surfaces (Figure S4 and Table S2). These surfaces have similar d_{gr} but smaller A_{gr}; therefore, mainly the A_{gb} increases, resulting in low R_1 and R_2

dx.doi.org/10.1021/ja5007417 | J. Am. Chem. Soc. 2014, 136, 6554−6557

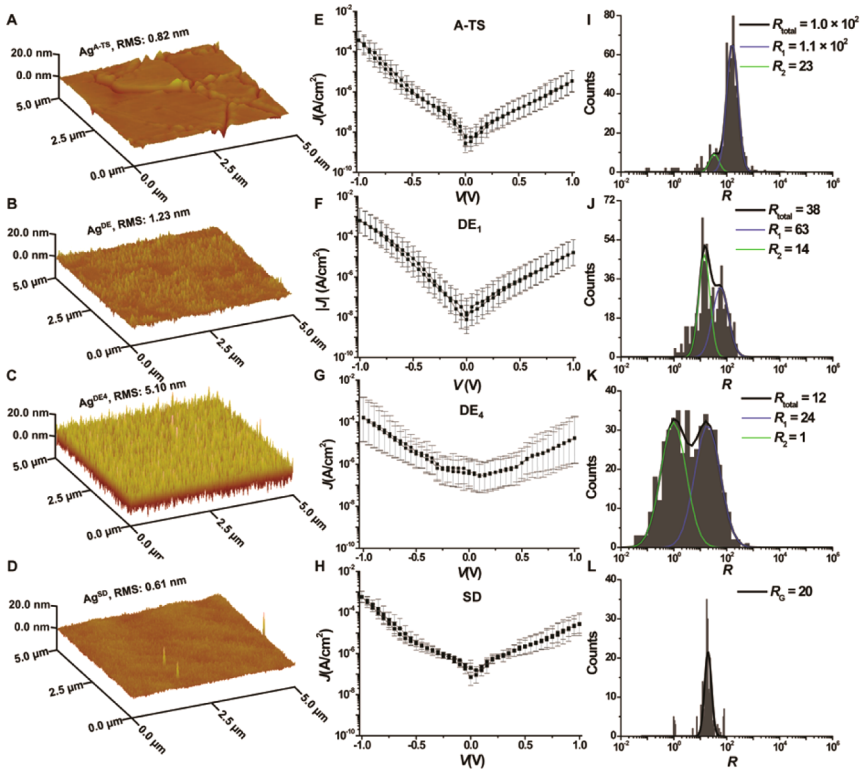

Figure 2. Atomic force micrographs of four of the seven types of Ag surfaces (A–D), average traces of the J–V plot of $SC_{11}Fc$ SAMs on the different surfaces (E–H), and histograms of R with Gaussian fits (I–K). See Figures S1–S3 for the full data set.

values. (iv) The positions of both R_1 and R_2 shift to lower values of R with increasing BV, but R_1 is always larger than R_2 (Figure S4 and Table S2). (v) The SD surfaces resulted in a distribution of R that consists of only one peak. Considering that these surfaces have very small grain boundary widths and the value of R_{tot} is very close to that of R_1 on rough surfaces, we believe that R_2 is absent.

These assignments of R_1 and R_2 correlate well with the data shown in Figure 3, which shows the yields of non-shorting junctions, reproducibility ($\sigma_{log,R}$), and R_{tot} as functions of BV. The dashed lines do not represent fits to any models and only serve to guide the eye. The value of R_{tot} decreases with increasing BV because both R_1 and R_2 decrease, and the more defective junctions also result in lower yields. The widths of the distributions of both R_1 and R_2 increase with increasing BV (Figure 3D), perhaps induced by other types of defects such as step-edges. For similar reasons, the values of R for Ag^{SD} surfaces are modest because the small grains contain large amounts of exposed grain boundaries but the grain widths (27 ± 2 nm) are modest and their depths (0.8 ± 0.1 nm; Table S1) are small relative to the length of the molecule.

Figure 3D shows the values of J measured at +1.0 V when the diodes are in the "off" state and block the current (the leakage current), and at −1.0 V when the diodes are in the "on" state and allow the current to pass through the junctions. The currents across the diodes in the "on" state are weakly dependent on the surface topography, while the leakage currents increase with increasing BV (Figure 3D). This observation indicates that the changes in the values of J do not originate from potential changes in the effective contact areas (except for junctions with Ag^{DE} electrodes; see below). The peak-to-valley roughness on a flat grain is about 0.12 nm, which is ~18 times smaller than the length of $SC_{11}Fc$ (2.15 nm based on CPK models). In contrast, the peak-to-valley roughness across grains (1.7–11.2 nm; Table

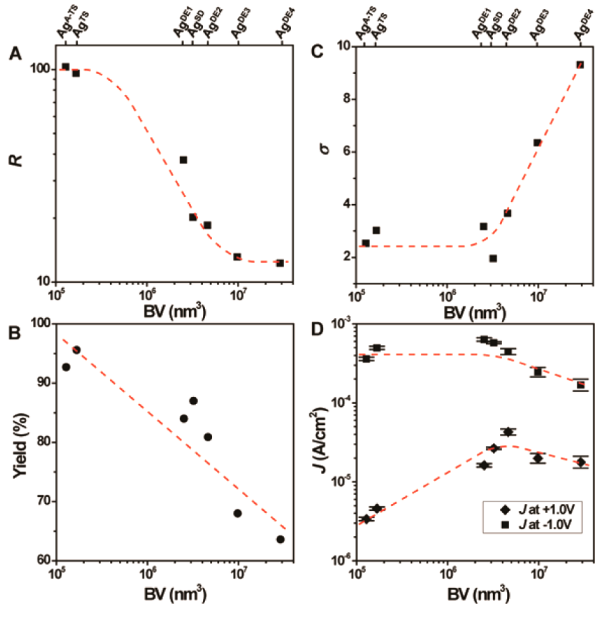

Figure 3. Plots of R_{tot} (A), yield (B), and log-standard deviations σ_{log} (C) of $\langle J \rangle$ at +1.0 and −1.0 V (D) against the bearing volume, BV. The dashed lines serve as guides to the eye.

S1) generally exceeds the length of the molecules, except for the Ag^{SD} surfaces. We believe that, due to the high surface tension of Ga_2O_3/EGaIn (~624 mN/m),[17] the top electrode cannot form conformal contacts to the grooves between two grains (as sketched in Figure 1C), but it forms contacts with the edges of the grains where the SAMs pack poorly. The Fc units are part of the tunneling barrier at positive bias, but at negative bias they act as sites to which charge can hop, while the alkyl chain is part of

dx.doi.org/10.1021/ja5007417 | J. Am. Chem. Soc. 2014, 136, 6554–6557

the tunneling barrier in both directions of bias.[14,15] Therefore, the surface topography has the largest impact on the leakage currents. We believe that the leakage currents increase by up to 2 orders of magnitude as a function of BV because small variations in the thickness of the SAMs cause large variations in the measured values of J when the diodes are in the "off" state (eq 2).

Figure 3D also shows that the values of J decrease with increasing BV values for junctions with Ag^{DE} electrodes. Whitesides et al. reported recently that the effective electrical contact area is lower than the geometrical contact area due to surface roughness.[18] We believe that these very rough surfaces reduce the effective contact are of the electrode with the SAMs because the top electrode cannot probe the voids due to its high surface tension, as indicated in Figure 1C. Although these uncertainties in the effective electrical contact areas influence the values of J, we do not expect them to be bias dependent, and consequently they do no affect R (eq 1).

These findings are in agreement with a previous report in which we showed that a small change of the average tilt angle of the Fc units (controlled via odd−even effects) resulted in a small difference in the packing energy of just 0.5 kcal/mol, and consequently in a 10-fold decrease of R because the leakage currents increased.[15] We expect that, at defect sites the SAMs are be disordered and the Fc units are randomly orientated and therefore cannot block the currents in the "off" state but still determine the total current that flows through the junctions. These loosely packed parts of the SAMs at defect sites cause defects in the junctions, resulting in broadened histograms of R (and even the appearance of a second peak), increased leakage currents, and lower yields of non-shorting junctions (Figure 3B).

In conclusion, the surface topography plays a crucial role in characteristics of molecular electronic devices. The rms surface roughness is not the only critical factor, but peak-to-valley roughness, numbers of grains, placement of the grains in the same plane, and width of the grooves between the grains are all important to obtain molecular junctions with well-defined supramolecular structures (see also Figures S5−S8). Only then will the device performance be optimal, because leakage currents are low with high yields in non-shorting junctions and good reproducibility. Surfaces with very small grains and low rms values have the highest reproducibility, because the depths of the grooves are small relative to the size of the molecules. Our findings indicate that the quality of the junctions could be further improved if the grain sizes exceed the geometrical junction area, or if the groove widths and depths are significantly smaller than the molecular dimensions.

By far, most studies have used electrodes prepared by direct metal deposition methods and only used rms values to judge the quality of these surfaces, but our results indicate that these surfaces result in diodes that do not perform well. Control over the surface topography is crucial to reduce leakage currents in molecular diodes, but we believe that our findings are generally applicable to other types of (bio)molecular electronic devices.

■ ASSOCIATED CONTENT

Supporting Information

Experimental details, surface analysis, J−V data, and statistical analysis. This material is available free of charge via the Internet at http://pubs.acs.org.

■ AUTHOR INFORMATION

Corresponding Author

chmnca@nus.edu.sg

Notes

The authors declare no competing financial interest.

■ ACKNOWLEDGMENTS

The authors thank the National Research Foundation of Singapore (No. NRF-RF2010-03 to C.A.N.) and Science Foundation Ireland (No. 11/SIRG/B2111 to D.T.).

■ REFERENCES

(1) (a) Mujica, V.; Ratner, M. A.; Nitzan, A. *Chem. Phys.* **2002**, *281*, 147. (b) McCreery, R. L.; Bergren, A. J. *Adv. Mater.* **2009**, *21*, 4303. (c) Rivnay, J.; Jimison, L. H.; Northrup, J. E.; Toney, M. F.; Noriega, R.; Lu, S. F.; Marks, T. J.; Facchetti, A.; Salleo, A. *Nat. Mater.* **2009**, *8*, 952. (d) Aradhya, S. V.; Venkataraman, L. *Nat. Nanotechnol.* **2013**, *8*, 399.

(2) Cademartiri, L.; Thuo, M. M.; Nijhuis, C. A.; Reus, W. F.; Tricard, S.; Barber, J. R.; Sodhi, R. N. S.; Brodersen, P.; Kim, C.; Chiechi, R. C.; Whitesides, G. M. *J. Phys. Chem. C* **2012**, *116*, 10848.

(3) (a) Tivanski, A. V.; Walker, G. C. *J. Am. Chem. Soc.* **2005**, *127*, 7647. (b) He, J.; Lindsay, S. M. *J. Am. Chem. Soc.* **2005**, *127*, 11932.

(4) (a) van der Molen, S. J.; Liljeroth, P. *J. Phys.: Condens. Matter* **2010**, *22*, 133001. (b) Simão, C.; Mas-Torrent, M.; Crivillers, N.; Lloveras, V.; Artés, J. M.; Gorostiza, P.; Veciana, J.; Rovira, C. *Nat. Chem.* **2011**, *3*, 359.

(5) Fan, F. R. F.; Yao, Y. X.; Cai, L. T.; Cheng, L.; Tour, J. M.; Bard, A. J. *J. Am. Chem. Soc.* **2004**, *126*, 4035.

(6) Beebe, J. M.; Kushmerick, J. G. *Appl. Phys. Lett.* **2007**, *90*, 083117.

(7) (a) Honciuc, A.; Jaiswal, A.; Gong, A.; Ashworth, H.; Spangler, C. W.; Peterson, I. R.; Dalton, L. R.; Metzger, R. M. *J. Phys. Chem. B* **2005**, *109*, 857. (b) Kitagawa, K.; Morita, T.; Kimura, S. *J. Phys. Chem. B* **2005**, *109*, 13906.

(8) Aviram, A.; Ratner, M. A. *Chem. Phys. Lett.* **1974**, *29*, 277.

(9) Shumate, W. J.; Mattern, D. L.; Jaiswal, A.; Dixon, D. A.; White, T. R.; Burgess, J.; Honciuc, A.; Metzger, R. M. *J. Phys. Chem. B* **2006**, *110*, 11146.

(10) (a) Elbing, M.; Ochs, R.; Koentopp, M.; Fischer, M.; von Hanisch, C.; Weigend, F.; Evers, F.; Weber, H. B.; Mayor, M. *Proc. Nat. Acad. Sci. U.S.A.* **2005**, *102*, 8815. (b) Díez-Pérez, I.; Hihath, J.; Lee, Y.; Yu, L. P.; Adamska, L.; Kozhushner, M. A.; Oleynik, I. I.; Tao, N. J. *Nat. Chem.* **2009**, *1*, 635.

(11) Weiss, E. A.; Chiechi, R. C.; Kaufman, G. K.; Kriebel, J. K.; Li, Z. F.; Duati, M.; Rampi, M. A.; Whitesides, G. M. *J. Am. Chem. Soc.* **2007**, *129*, 4336.

(12) Yuan, L.; Jiang, L.; Zhang, B.; Nijhuis, C. A. *Angew. Chem., Int. Ed.* **2014**, *53*, 3377.

(13) Nijhuis, C. A.; Reus, W. F.; Whitesides, G. M. *J. Am. Chem. Soc.* **2009**, *131*, 17814.

(14) (a) Nijhuis, C. A.; Reus, W. F.; Whitesides, G. M. *J. Am. Chem. Soc.* **2010**, *132*, 18386. (b) Nijhuis, C. A.; Reus, W. F.; Barber, J. R.; Dickey, M. D.; Whitesides, G. M. *Nano Lett.* **2010**, *10*, 3611.

(15) Nerngchamnong, N.; Yuan, L.; Qi, D. C.; Li, J.; Thompson, D.; Nijhuis, C. A. *Nat. Nanotechnol.* **2013**, *8*, 113.

(16) Vj, L.; Kobayashi, N. P.; Islam, M. S.; Wu, W.; Chaturvedi, P.; Fang, N. X.; Wang, S. Y.; Williams, R. S. *Nano Lett.* **2009**, *9*, 178.

(17) Chiechi, R. C.; Weiss, E. A.; Dickey, M. D.; Whitesides, G. M. *Angew. Chem., Int. Ed.* **2008**, *47*, 142.

(18) Simeone, F. C.; Yoon, H. J.; Thuo, M. M.; Barber, J. R.; Smith, B.; Whitesides, G. M. *J. Am. Chem. Soc.* **2013**, *135*, 18131.